Electronic Supplementary Information

Environmentally sustainable moisture energy harvester with chemically networked cellulose nanofiber

EunAe Shin,[a,b] Gwanho Kim,[a] Kaiying Zhao,[a] Guangtao Zan,[a] HoYeon Kim,[a] Shengyou Li,[a] Junhyuk Lee,[b] DongHo Kang,[b] Jin Woo Oh,[a] Jeyoung Jung,[b] Jin Kie Shim,[*b] and Cheolmin Park[*a]

[a] Department of Materials Science and Engineering, Yonsei University, Yonsei-ro 50, Seodaemun-gu, Seoul, 03722, Korea.

[b] Korea Packaging Center, Korea Institute of Industrial Technology, Bucheon, 14449, Republic of Korea.

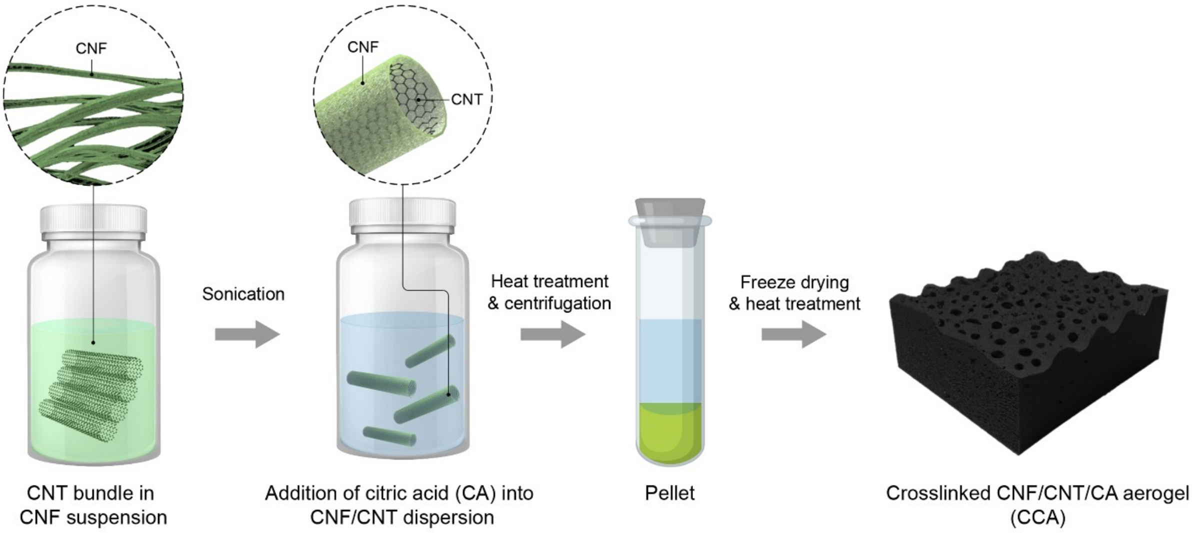

Fig. S1 Schematic diagram of CCA fabrication.

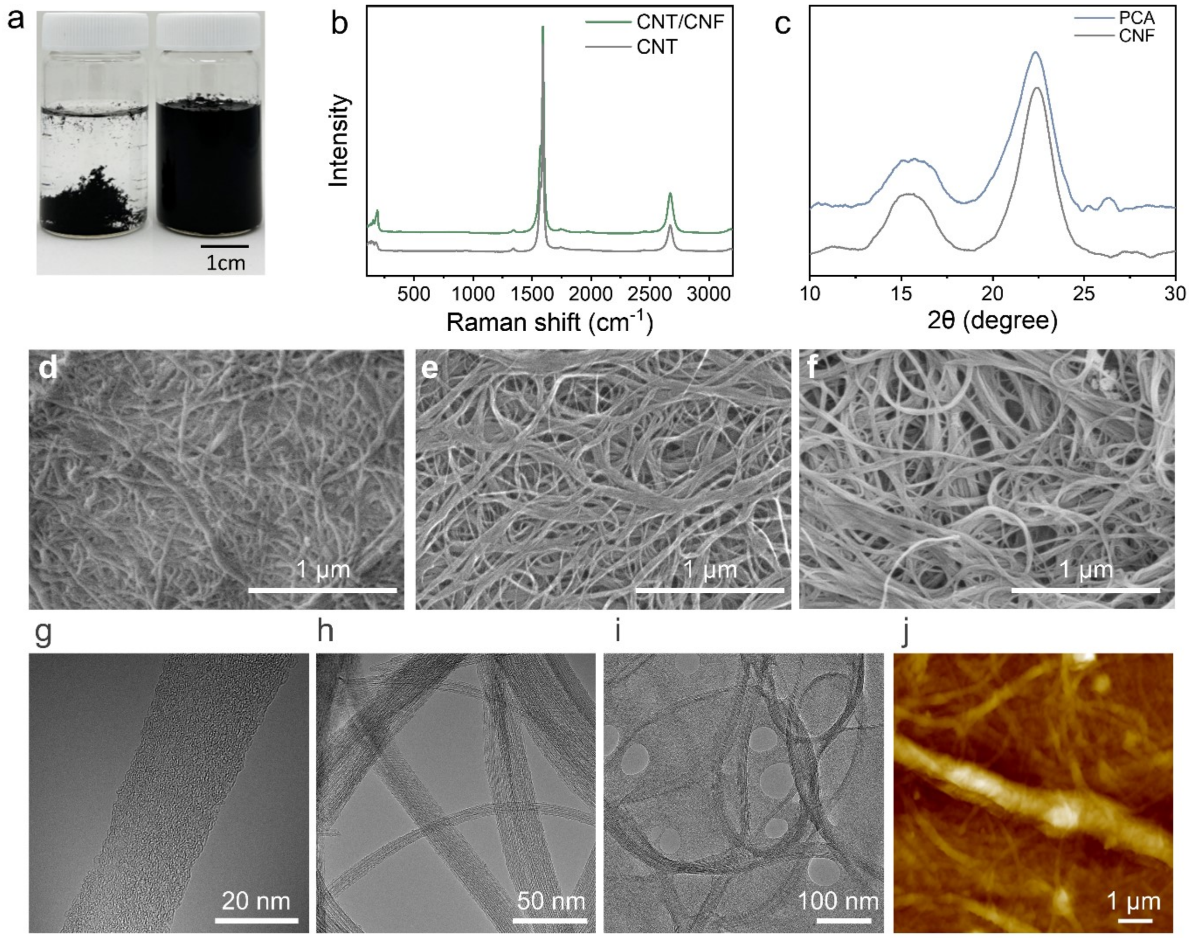

Fig. S2 a) Photo of CNT in DI water (left) and CNT with CNF in DI water (right) after sonication treatment. b) Raman spectra of pristine CNT and CNT/CNF composite. c) XRD pattern of CNF and CNT/CNF composite. SEM images of d) CNF, e) CNT, and f) CNT/CNF aerogel. TEM images of g) CNF, h) CNT, and i) CNT/CNF. j) AFM image of CNT/CNF.

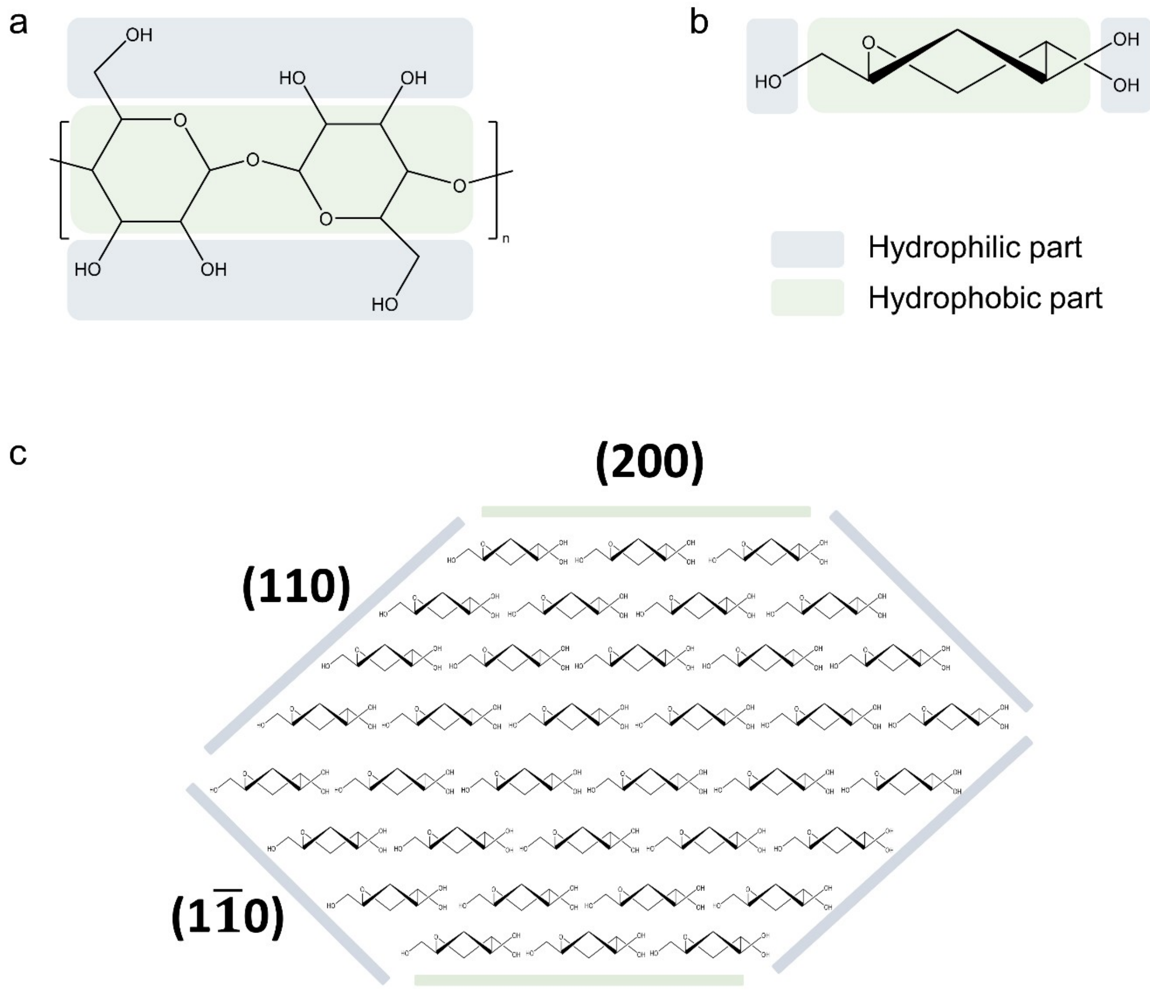

Fig. S3 Views of cellulose: a) top, b) side of cellulose chain. c) molecular model of cellulose chains.

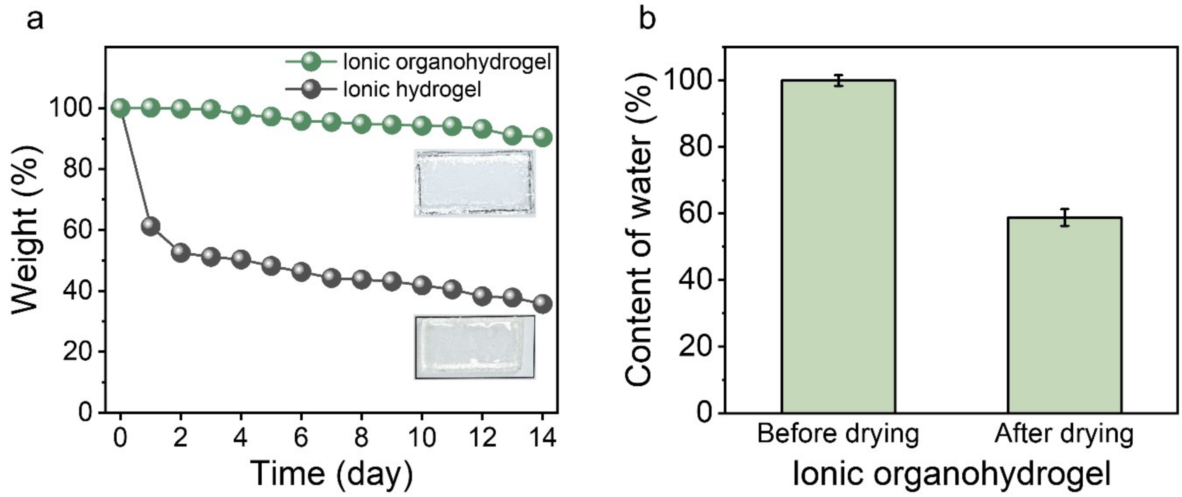

Fig. S4 a) Water retention of ionic hydrogel and ionic organohydrogel and b) water content in ionic organohydrogel before and after drying.

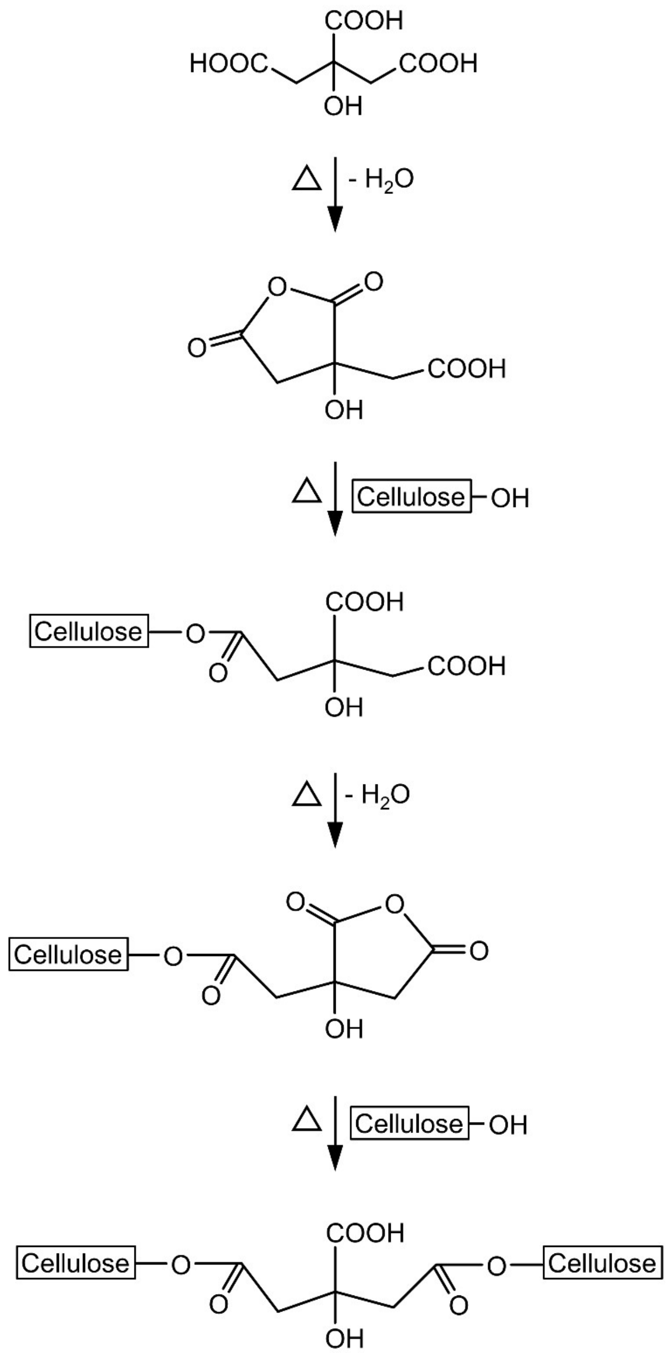

Fig. S5 Proposed crosslinking reaction mechanism of citric acid with cellulose.

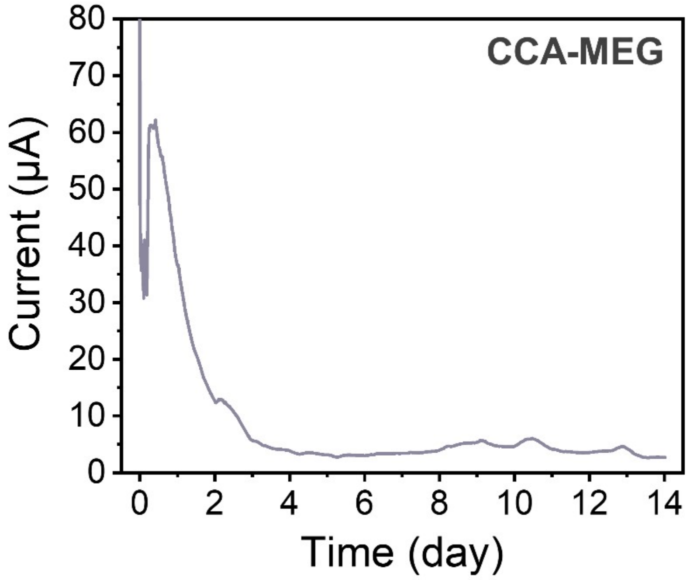

Fig. S6. Plot of continuous I_{sc} of CCA-MEG for 2 weeks.

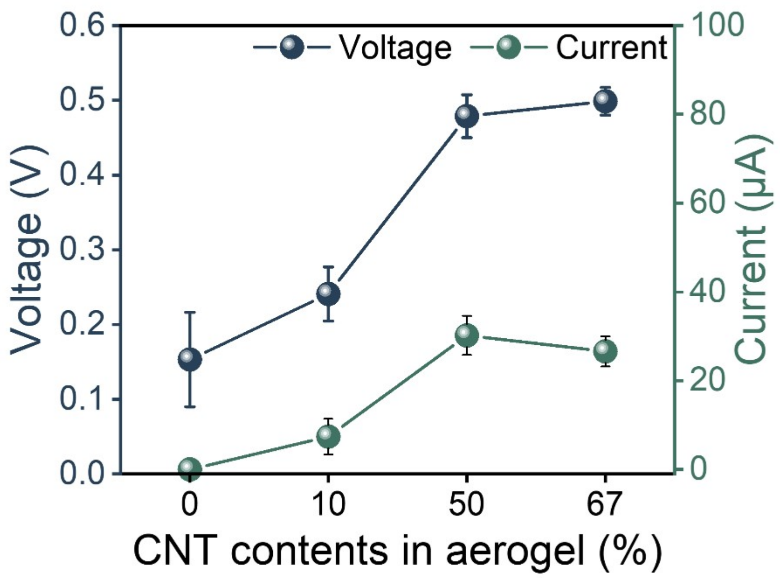

Fig. S7 V_{oc} and I_{sc} corresponding to the ratio of CNT in aerogel of PCA-MEG: a) 0%, b) 10%, c) 50%, and d) 67%.

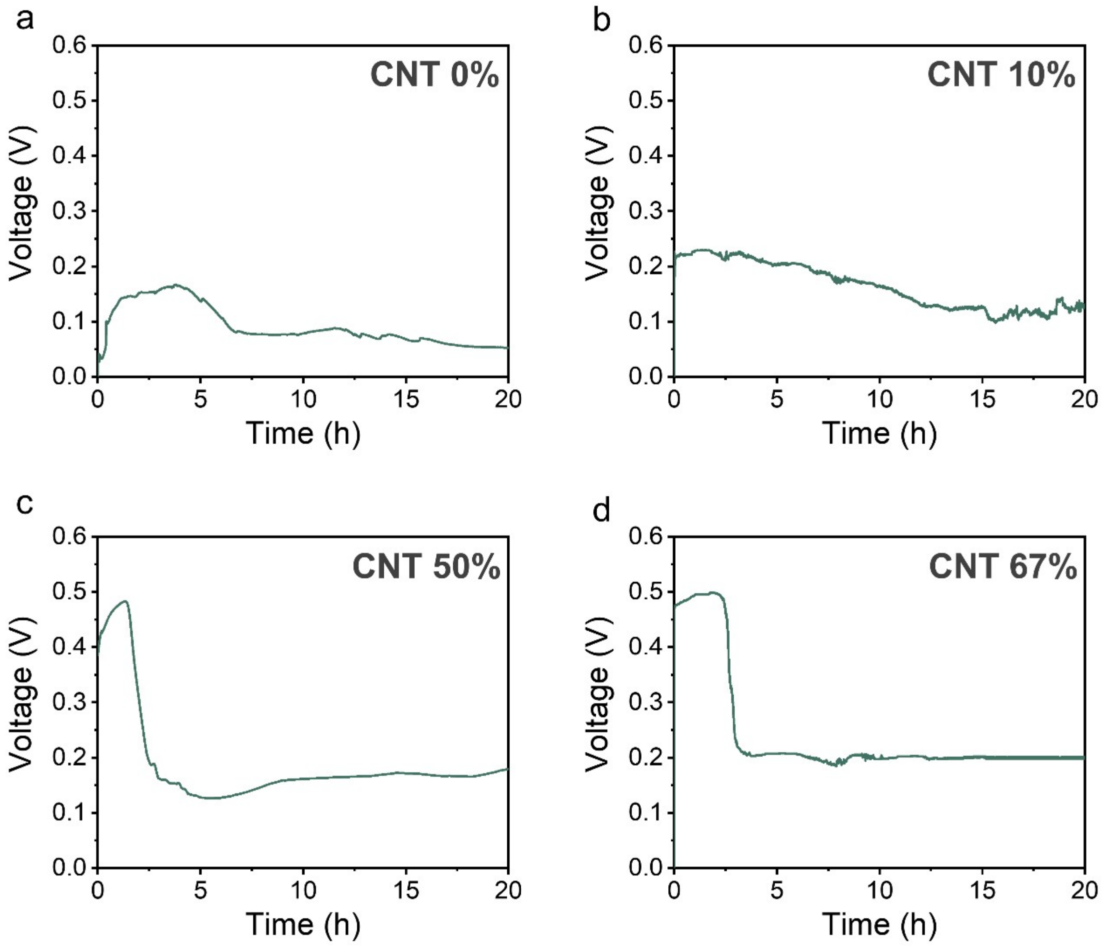

Fig. S8 Plot of V_{oc} corresponding to the ratio of CNT in aerogel of PCA-MEG: a) 0%, b) 10%, c) 50%, and d) 67%.

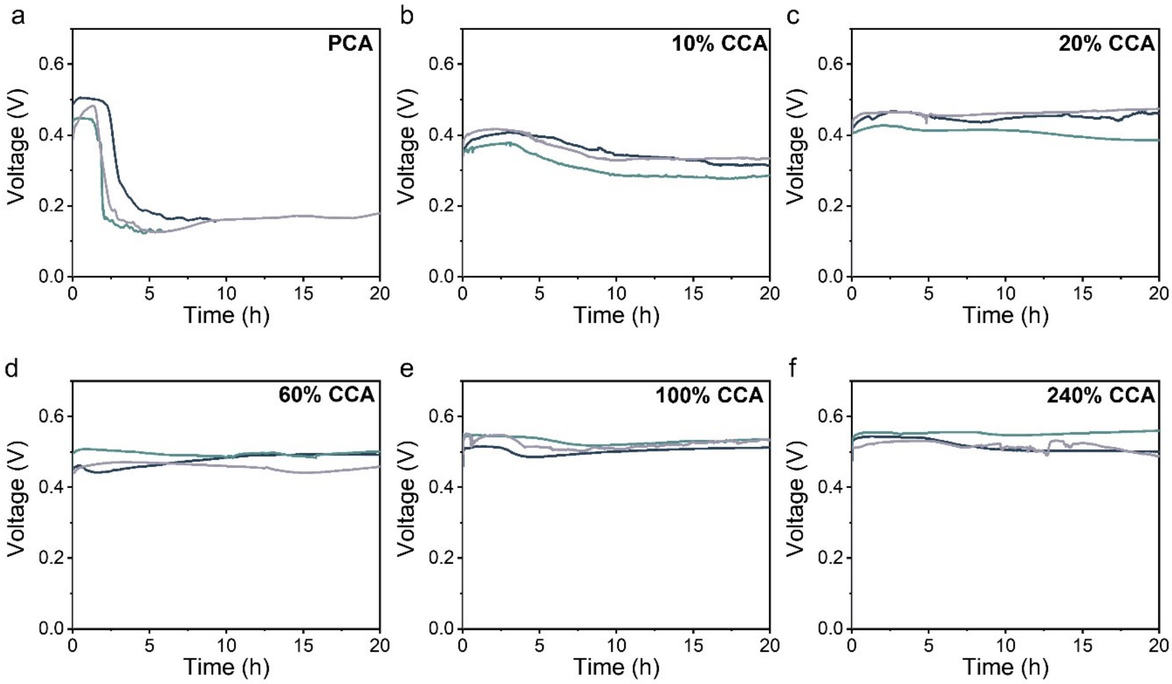

Fig. S9 Plot of continuous voltage output of a) PCA-MEG and b–f) CCA-MEG with varying CA content for a long duration. b) 10%, c) 20%, d) 60%, e) 100%, and f) 240% CA added by weight of CNF (20 °C and RH 30%).

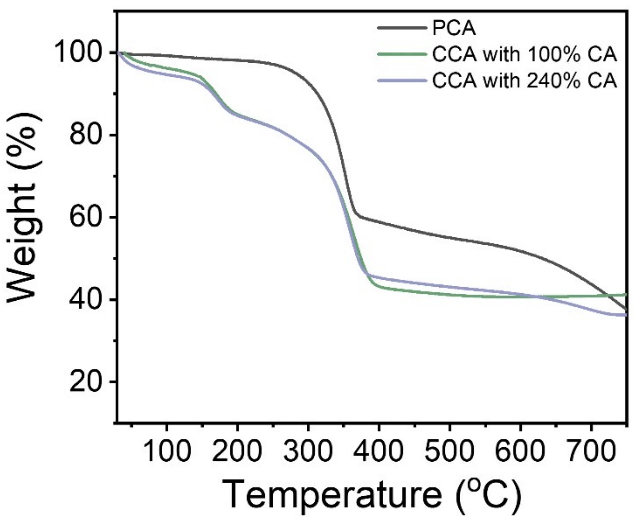

Fig. S10 Thermogravimetric analysis (TGA) of PCA and CCA with 100% and 240% CA.

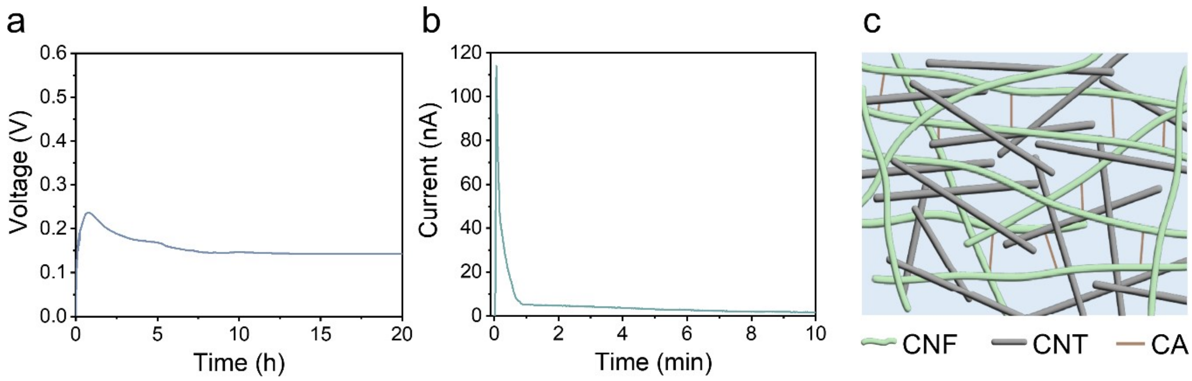

Fig. S11 a) V_{oc} and b) I_{sc} of MEG using crosslinked CNF/CA aerogel without CNT and c) the scheme of network formed by CNTs and crosslinked CNFs.

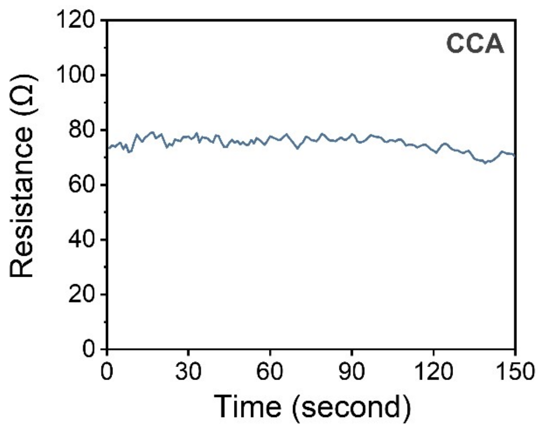

Fig. S12 Resistance of CCA incorporated with 100% CA.

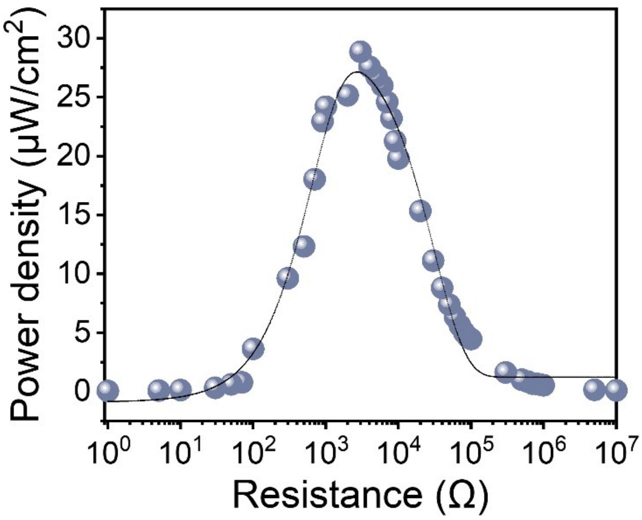

Fig. S13 Maximum power density obtained by measuring the V_{oc} and I_{sc}.

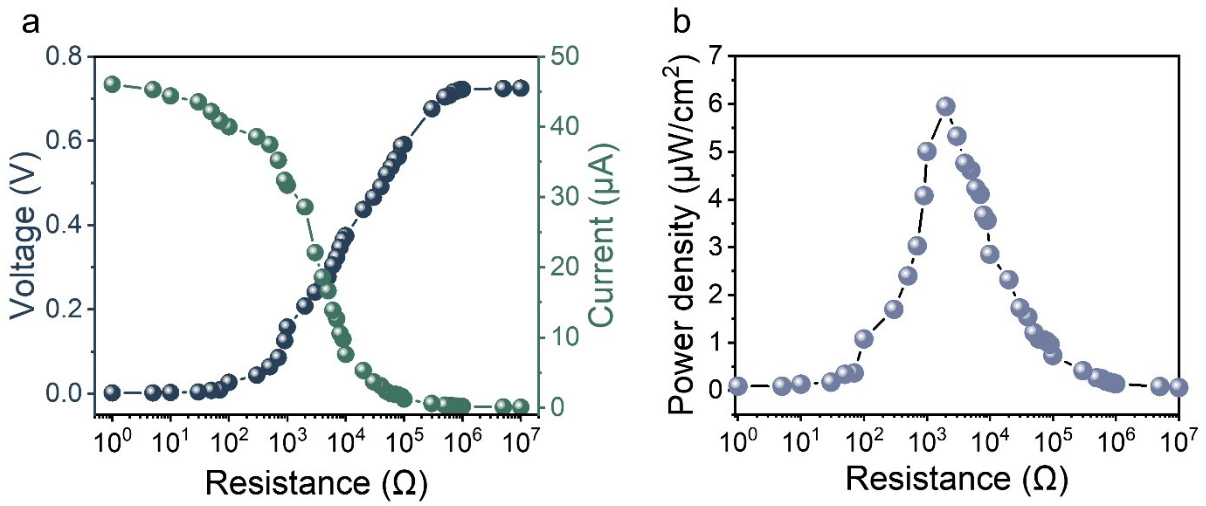

Fig. S14 a) V_{oc} and I_{sc} of the CCA-MEG af 5 minutes after measurement with external resistance and b) power density calculated by measuring V_{oc} and I_{sc} measured at 5 minutes operation.

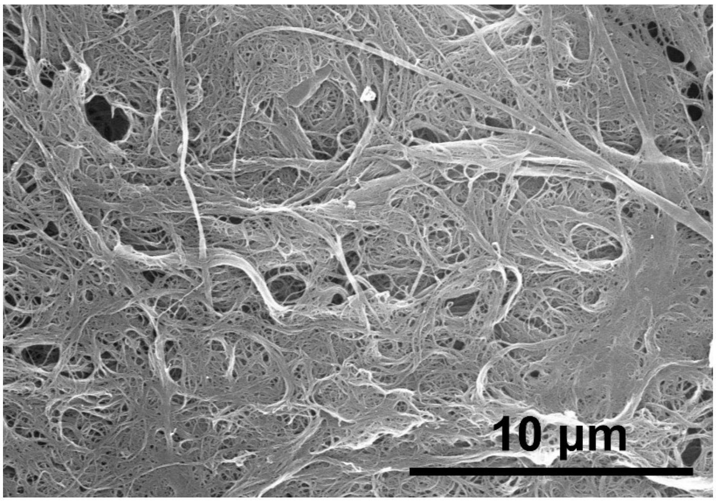

Fig. S15 A SEM image of CCA after 350 h power generation.

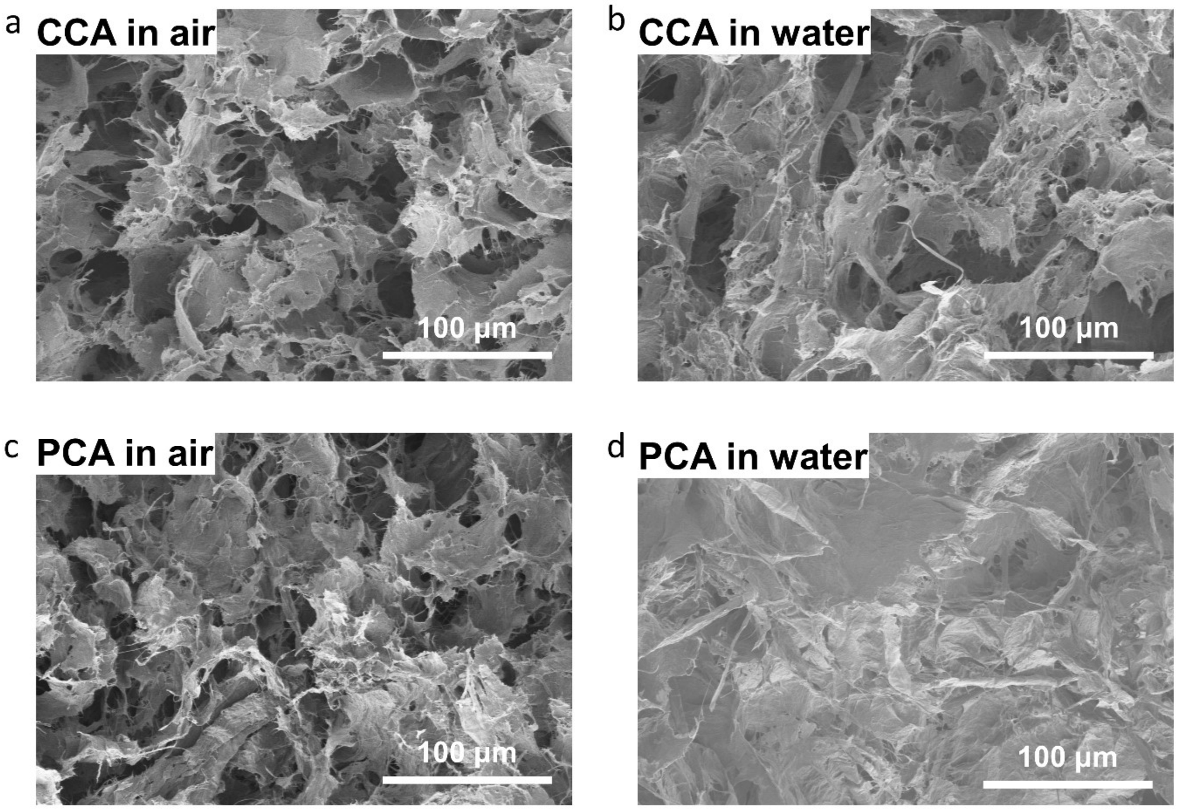

Fig. S16 SEM images of a) CCA in air, b) CCA in water, c) PCA in air and d) PCA in water.

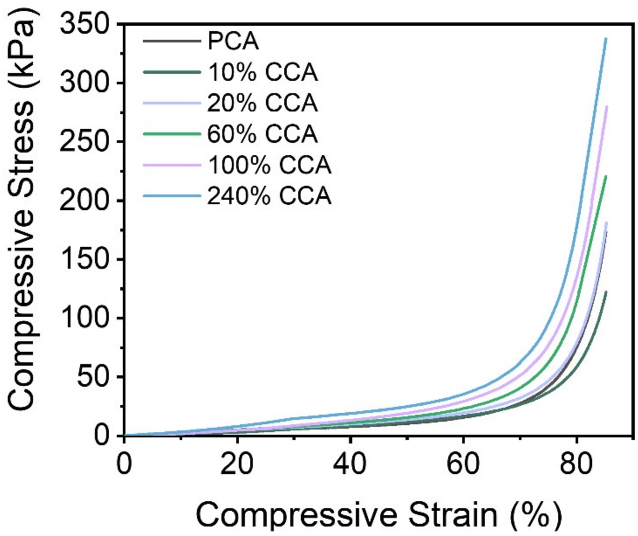

Fig. S17 Plot of compressive strain–stress curve with PCA and CCA depending on CA content.

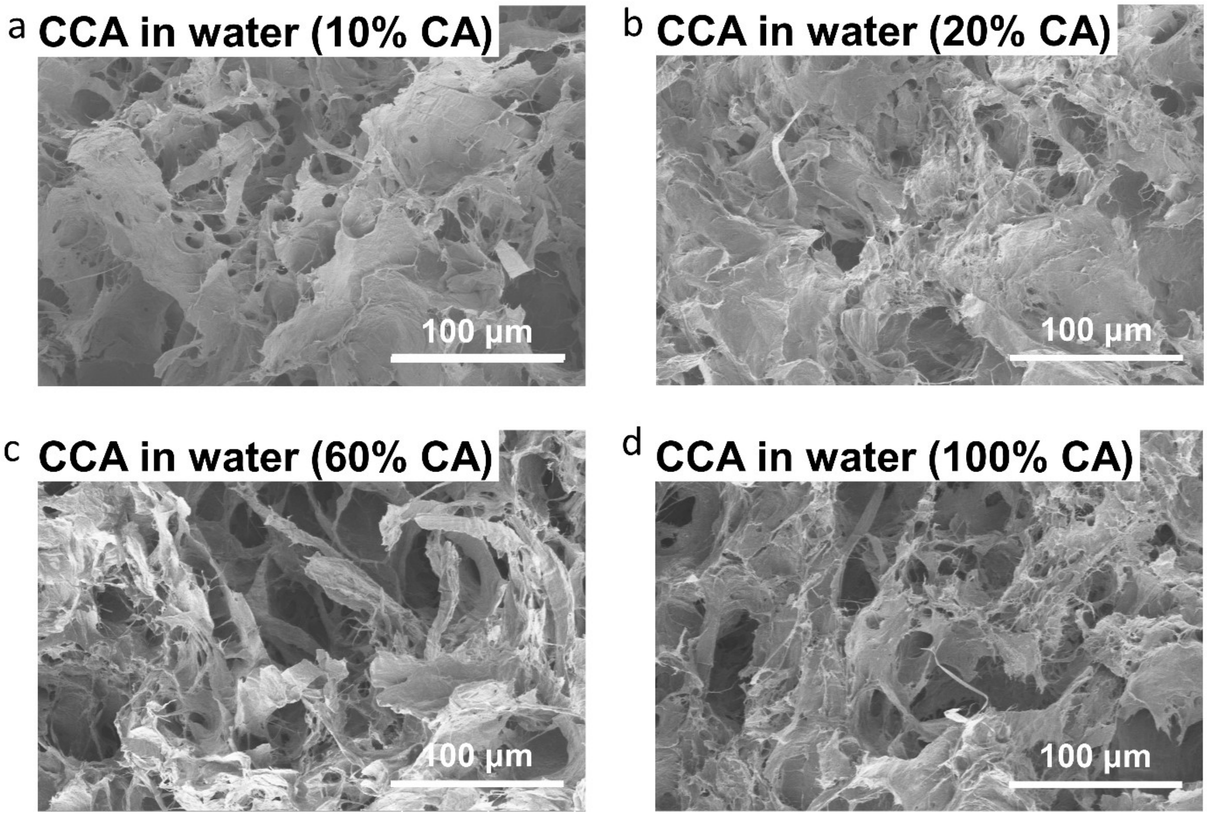

Fig. S18 SEM images of a) CCA with 10% CA, b) 20% CA, c) 60% CA and d) 100% CA after immersed in water.

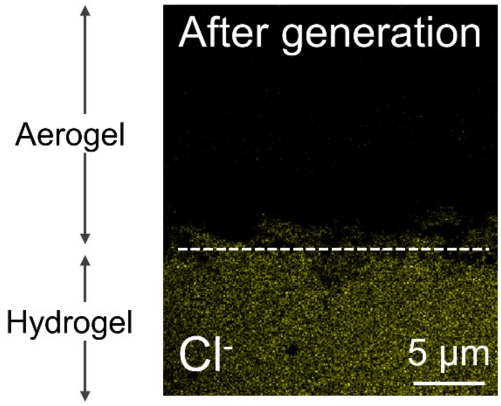

Fig. S19 EDS mapping data of Cl^- ions after generation in CCA-MEG.

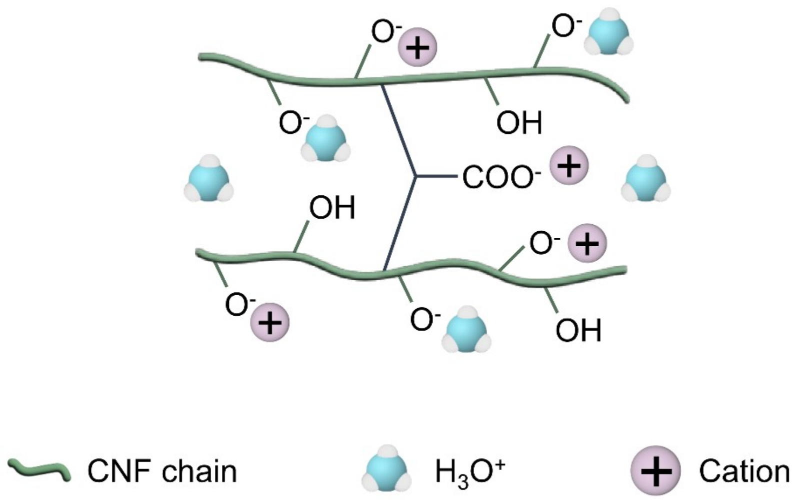

Fig. S20 The schematic illustration of the ionic dissociation contributed by the surface functional groups of CNF.

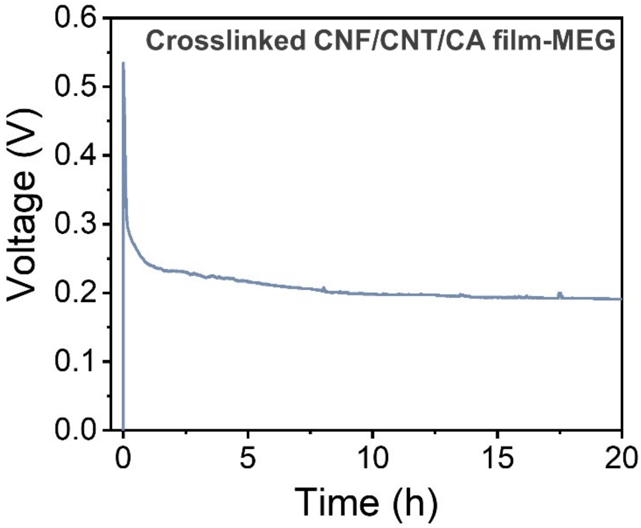

Fig. S21 Plot of continuous V_{oc} of crosslinked CNF/CNT/CA film-MEG.

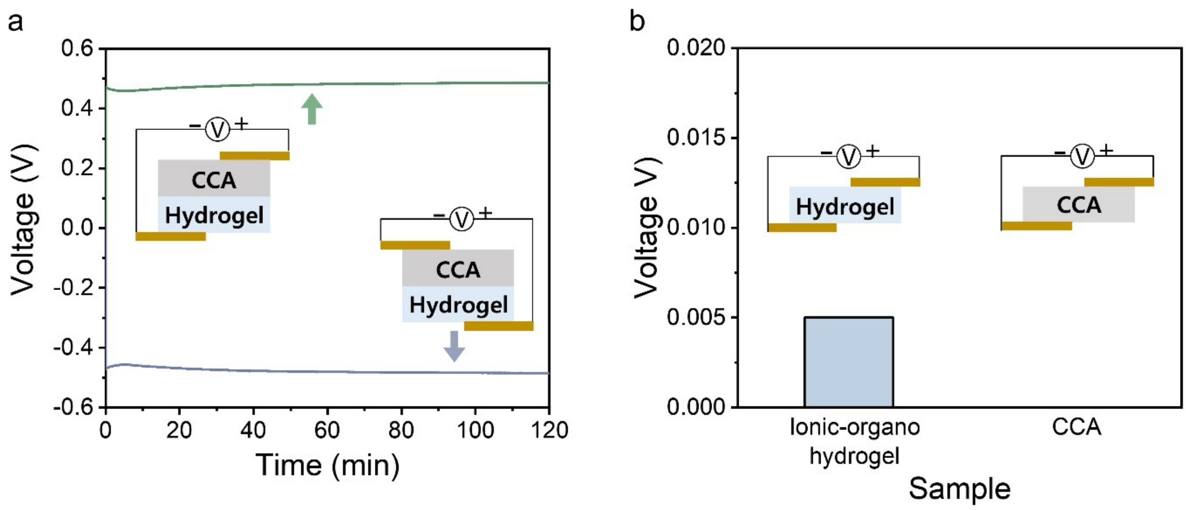

Fig. S22 a) Continuous V_{oc} of CCA-MEG devices with reversed connection, and b) V_{oc} of MEG device with CCA and ionic organohydrogel.

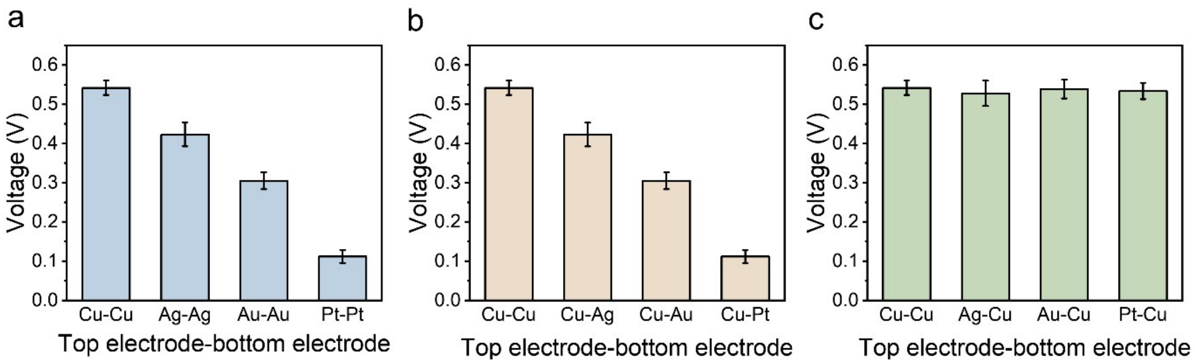

Fig. S23 V_{oc} values of CCA-MEGs with various combinations of contact electrodes. a) V_{oc} values when the top and bottom electrodes are of the same materials. b) V_{oc} values when the bottom electrode is Cu, Ag, Au, and Pt with a top Cu electrode. c) V_{oc} values when the top electrode is Cu, Ag, Au, and Pt with the bottom electrode is Cu.

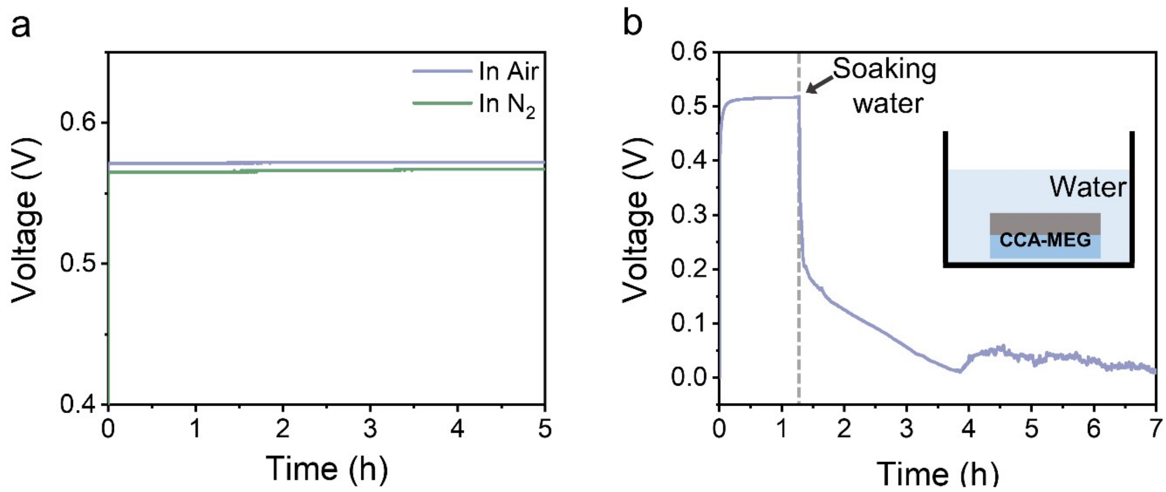

Fig. S24 V_{oc} of a CCA-MEG in different atmospheres (air and N_2) and b) V_{oc} of a CCA-MEG in water.

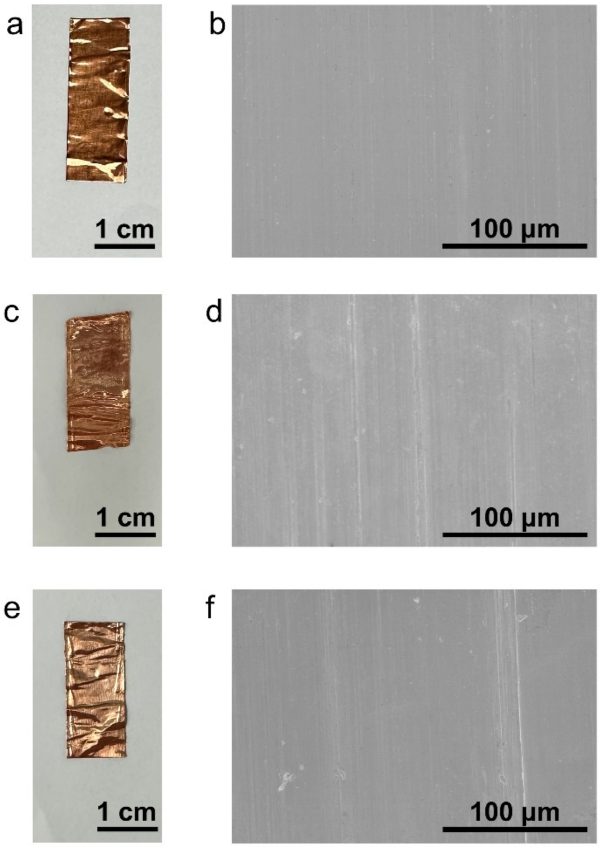

Fig. S25 a) A photograph of an initial Cu electrode. b) A SEM image of an initial Cu electrode. c) A photograph of a Cu electrode after used for top electrode in a CCA-MEG tested for two months. d) A SEM image of a Cu electrode after used for top electrode in CCA-MEG tested for two months. e) A photograph of a Cu electrode after used for bottom electrode in CCA-MEG tested for two months. f) A SEM image of a Cu electrode after used for bottom electrode in CCA-MEG tested for two months.

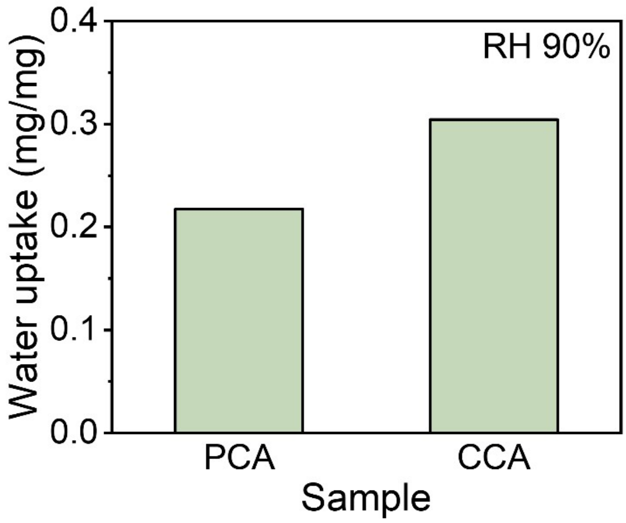

Fig. S26 Equilibrium moisture uptake of PCA and CCA at RH 90%.

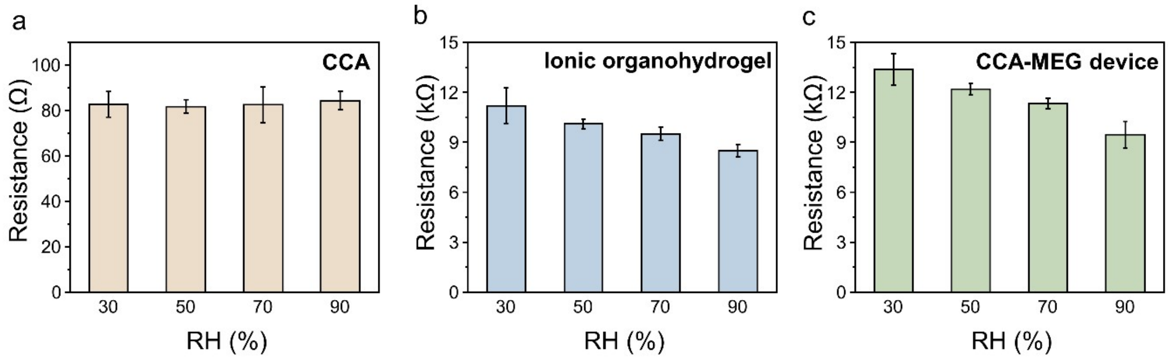

Fig. S27 The resistance of a) CCA, b) ionic hydrogel and c) CCA-MEG device at various RH.

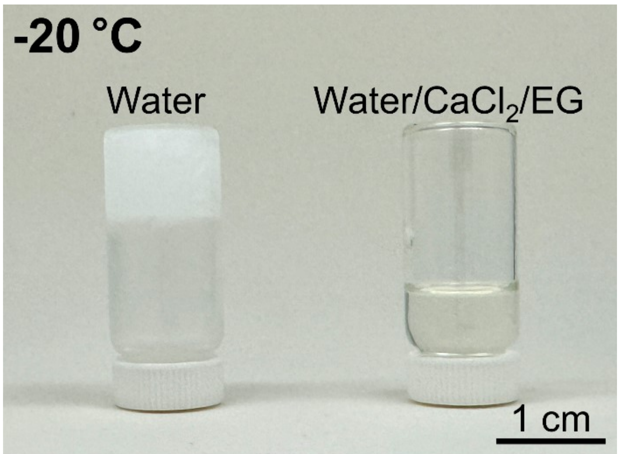

Fig. S28 Photograph of water (left) and water/$CaCl_2$/Ethylene glycol solution (right) at −20 ^oC.

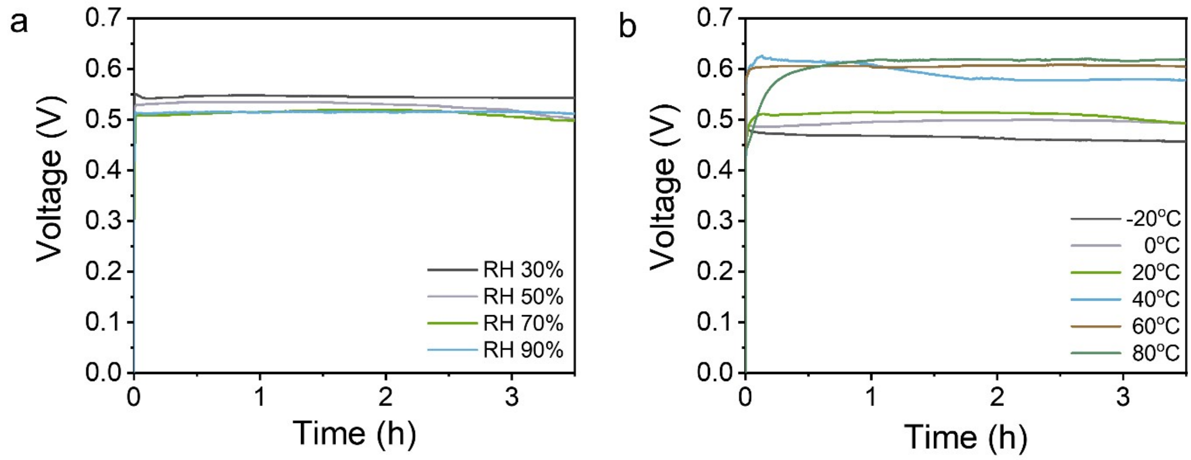

Fig. S29 Plot of continuous V_{oc} of CCA-MEG with a) RH at 20 °C and b) temperature at 30% RH.

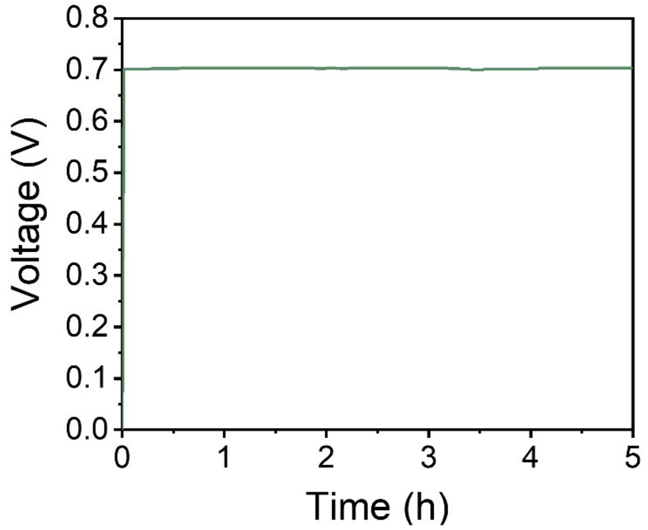

Fig. S30 Continuous V_{oc} with CCA-MEG utilizing an ionic organohydrogel with a concentration of 2M ions and a thickness of 3 mm.

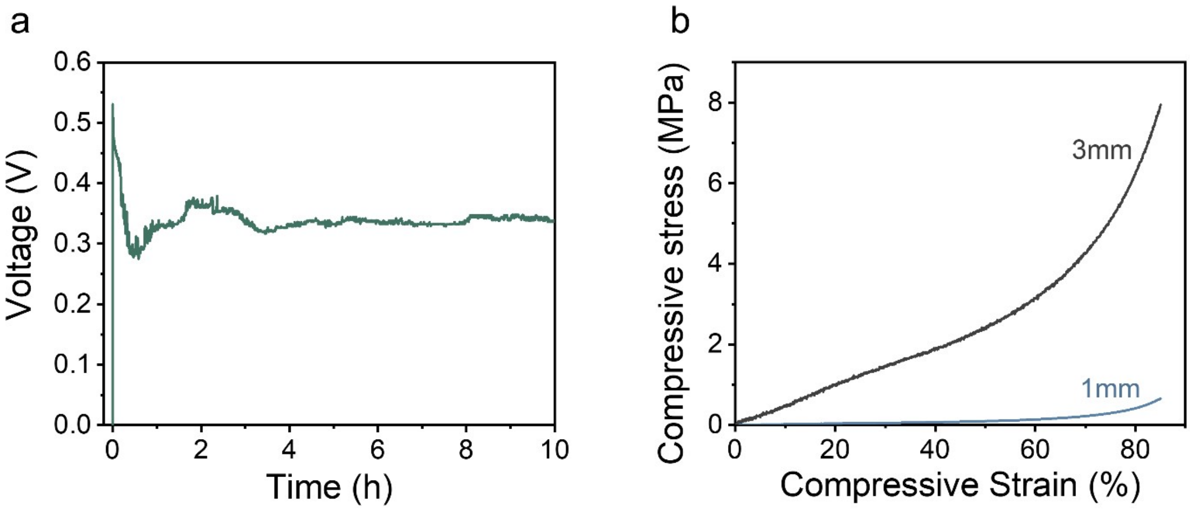

Fig. S31 a) Continuous V_{oc} of CCA-MEG with 1 mm thick aerogel and b) compressive strain-stress curve for aerogels with thickness of 1 mm and 3 mm.

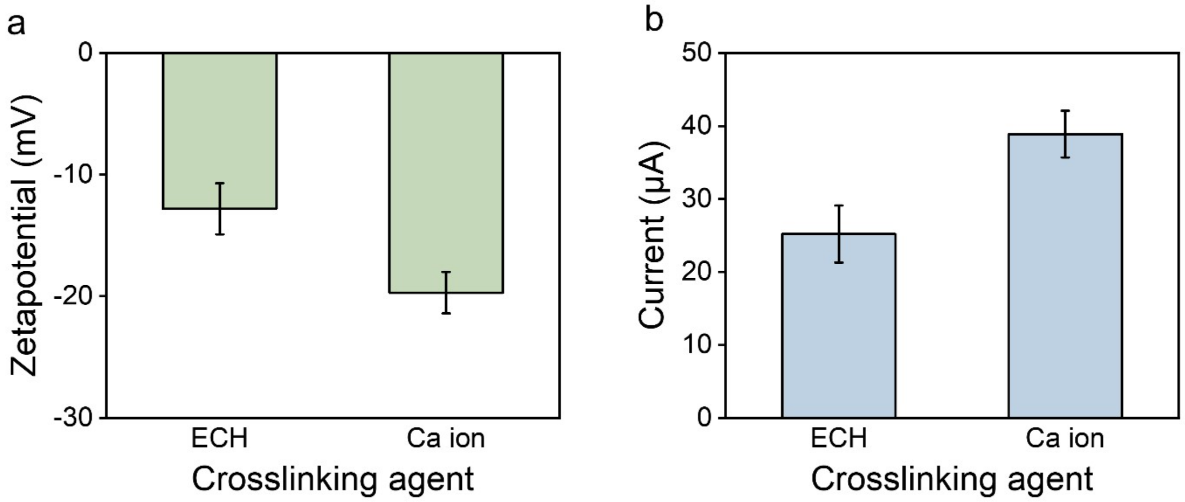

Fig. S32 a) Zetapotential and b) I_{sc} of crosslinked CNF/CNT suspension by ECH and calcium ion.

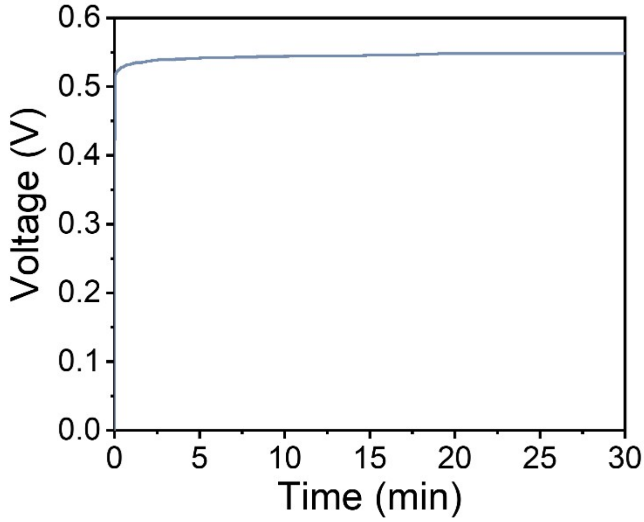

Fig. S33 V_{oc} of CCA-MEG using the original CCA and the reused ionic organohydrogel.

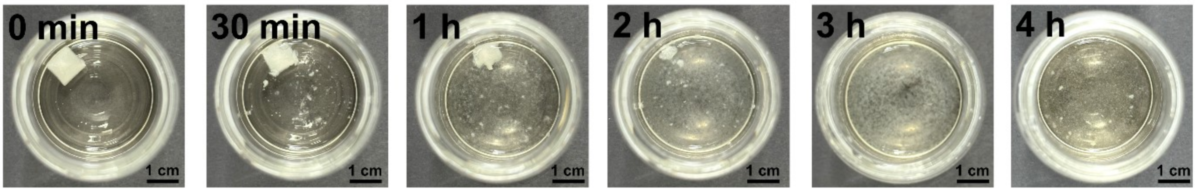

Fig. S34 Photographs of the degradation of crosslinked CNF aerogel in the cellulase solution.

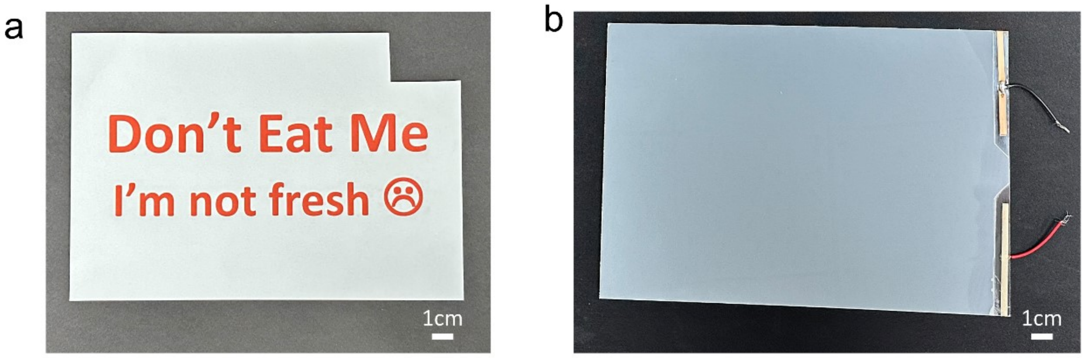

Fig. S35 Photograph of a) warning label and b) PDLC film for smart package.

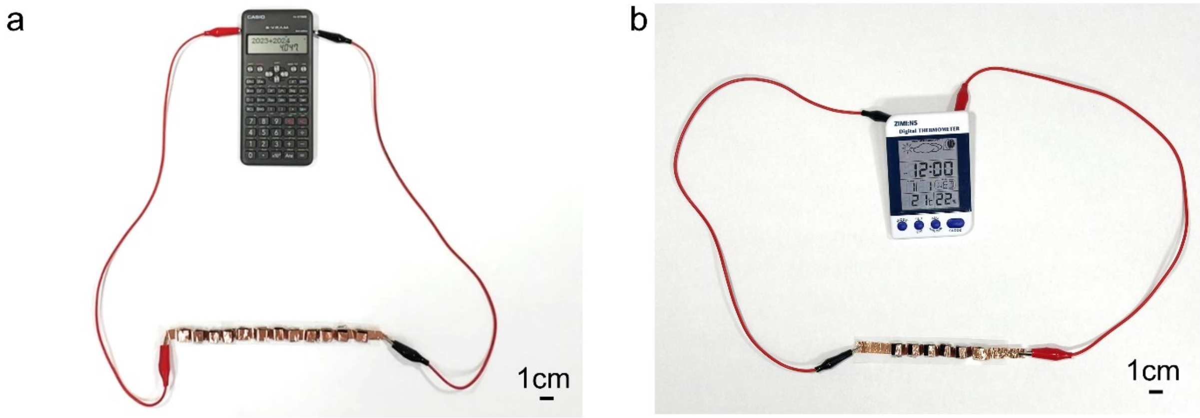

Fig. S36 a) Photograph of a commercial calculator operated by 12 CCA-MEG units in a series connection. b) Photograph of a commercial thermo-hygrometer operated using 5 CCA-MEG units in a series connection.

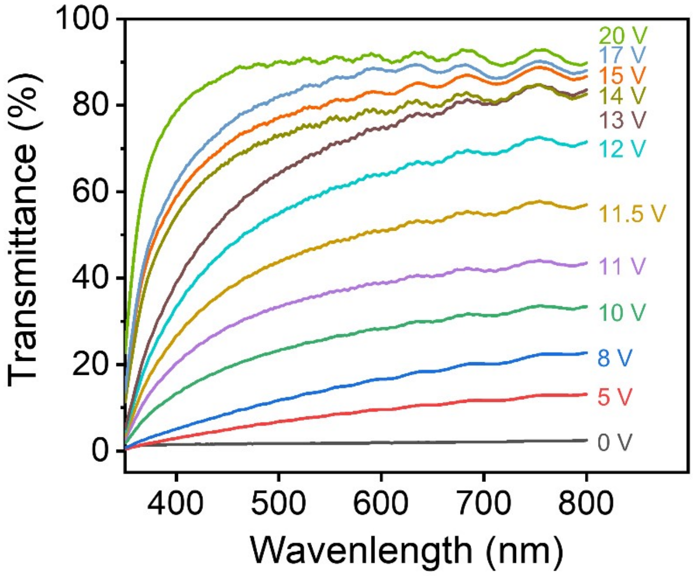

Fig. S37 Transmittance of the PDLC film at various voltages.

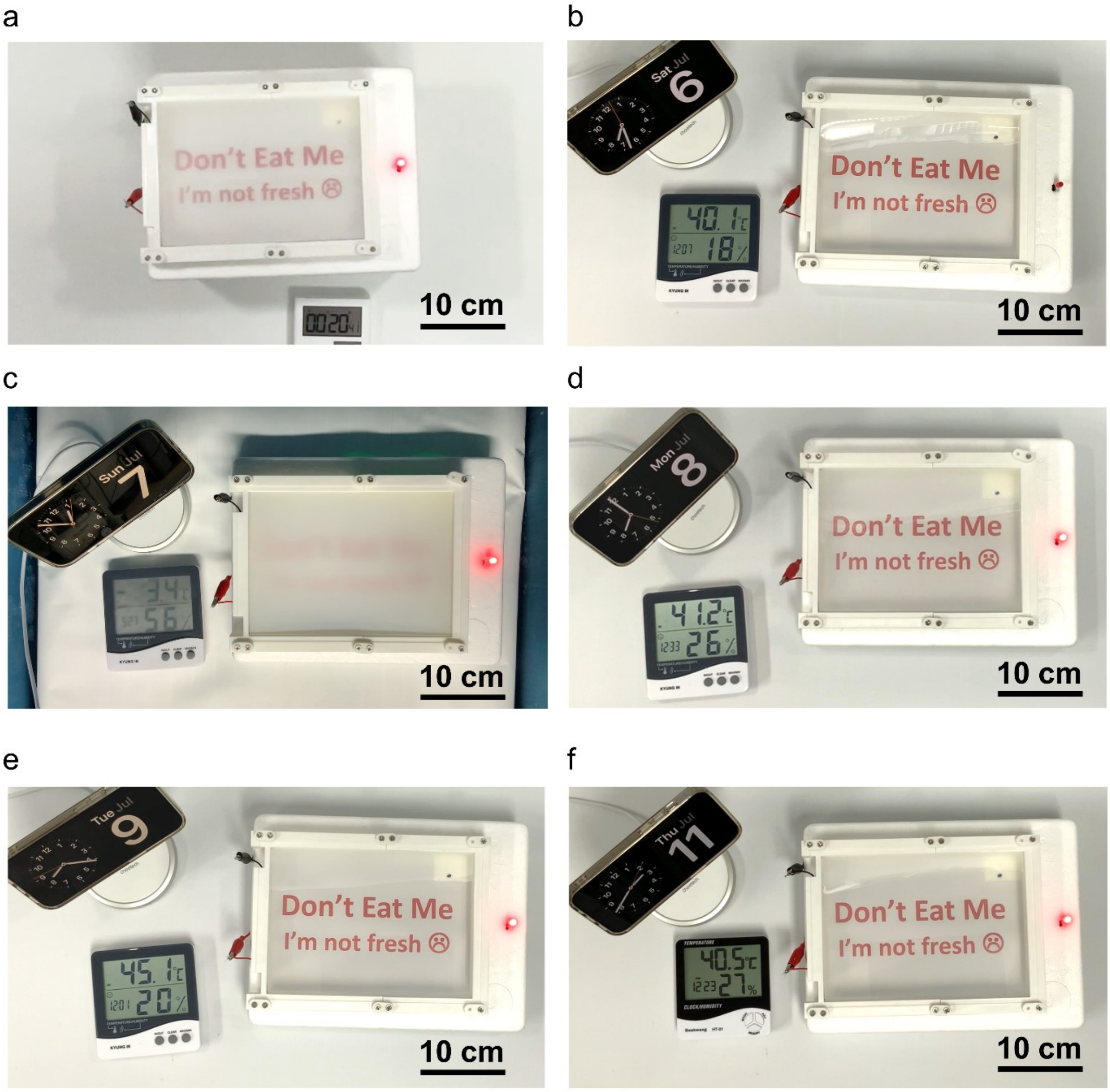

Fig. S38 Photographs of self-powered MEG based smart package a) after 20 minutes continuous operation, b) after 1 day operation at 40 °C, c) after 1 day operation at -3 °C, d) after 2 days of operation at 45 °C again, e) after re-connection from 3 days of first operation, and f) after on/off switching from 5 days of first operation.

Table S1 Summary of output performances of biopolymer based MEG devices.

Key material	Type	Voltage (V)	Time (h)	Current (μA)	Power density (μW/cm²)	Reference
CNF/CNT/Citric acid	Aerogel	0.25	> 350	38	28	This work
Carboxymethyl cellulose	Film	0.3	8.3	0.015	0.0025	1
Cellulose acetate	Electrospun membrane	0.11	0.8	80	0.0084	2
TEMPO-CNF	Aerogel	0.115	167	0.022	0.0024	3
TEMPO-CNF/Quatern-CNF bilayer	Ionic aerogel	0.385	0.25	0.015	0.0017	4
Cellulose/PEDOT:PSS	Wood	0.7	0.8	11	0.198	5
Cellulose acetate with salt	Electrospun membrane	1.1	0.17	3.5	2.45	6
Delignified wood	Aerogel	0.55	11	320	6.75	7
COF-Cellulose Aerogels	Aerogel	0.3	5	0.34	0.044	8
Carbon black coating on cellulose acetate microfiber	Microfiber cylinder	0.1604	0.5	100	4.58	9
CNT/regenerated cellulose	Fiber	0.78	0.8	0.17	0.0035	10
LiCl-cellulose paper/ carbon black paper bilyaer	Paper	0.803	240	3.7	0.67	11
Cellulose filter paper/carbon	Paper	0.668	168	1.03	2.63	12
CNT/CMC/CNF	Aerogel	0.84	1	6.4	0.871	13
MWNT/cellulose	Film	0.275	45	2.21	0.163	14
MXene/Paper/Citric acid	Paper	0.25	150	7.6	2.1	15
MoS_2-functionalized filter paper	Paper	0.302	0.1	21.1	5	16
MOF/modified NFC	Aerogel	0.65	0.7	3.7	1.12	17
AgNW coating on cellulose acetate	Membrane	0.25	15	0.12	0.4	18
Protein wires	Film	0.5	1500	17	5.00	19
β-lactoglobulin (milk protein)	Nanofibril	0.65	240	2.9	9.02	20
Gelatin protein	Film	0.71	0.003	7.77	5.5	21
Protein/PEG	Film	1.45	3	113	11.6	22
Microorganism (G.sulfurreducens)	Film	0.5	700	2	1	23
Microorganism (G.sulfurreducens)	Film	0.3	10	13	5.1	24
Nb_2CT_x/sodium alginate	Film	0.5	720	1.6	0.5	25
Oxi-silk/AgNP	Fiber	0.28	0.28	0.19	0.05	26
Sodium alginate/CNT	Fiber	0.38	36	1.74	9.5	27
Cationic silk	Nanofibril	0.12	0.056	0.11	0.01	28

Table S2 Summary of output performances of recent MEG devices.

	Key material	Voltage (V)	Time (h)	Current (μA)	Power density (μW/cm^2)	Recycle possibility	Reference
Biomaterial	CNF/CNT/Citric acid	0.25	> 350	38	28.9	O	This work
	Delignified wood	1.1	11	320	6.75	O	7
	Cellulose filter paper/carbon	0.803	168	1.03	2.63	O	12
	Protein wires	0.5	1500	17	5	O	19
	Milk protein	0.65	240	2.9	9.02	O	20
	Gelatin	0.71	0.003	7.77	5.5	O	21
	Microorganism	0.3	10	13	5.1	O	24
	Nb_2CT_x/sodium alginate	0.5	720	1.6	0.5	O	25
	Oxi-silk/AgNP	0.28	0.28	0.19	0.05	O	26
	Sodium alginate/CNT	0.38	36	1.74	9.5	O	27
	Cationic silk	0.12	0.056	0.11	0.01	O	28
Synthetic Polymer	PSSA:PDDA/Al	1.1	13.9	11.3	2.60	X	29
	PAN:PSSA	1.1	11.1	1.35	1.48	X	30
	PAM:AMPS hydrogel	0.81	3	480	53.30	X	31
	PSS membrane	0.8	12	120	13.00	X	32
	PAN-PVP-Ag core-shell yarn	0.8	8.3	14.3	0.61	X	33
	PVA/PSS textile	1	5	1.7	0.10	X	34
Carbon	Porous GO membrane	0.45	0.13	0.9	2.02	X	35
	CNT/AAO/In-Ga	1.1	720	1.5	1.30	X	36
	GO/PAAS composite	0.6	120	12	0.07	X	37
	GO-CNT	0.76	24	73	15.80	X	38
	GO	1.39	11	120	110.00	X	39
	Carbon black cotton	0.3	2.5	50	0.70	X	40
	CNT/Mxene	0.36	0.14	520	1.55	X	41
Inortanic materials	TiO_2 wire	0.52	0.04	8	4.00	X	42
	SiO_2/Graphene sphere	0.34	5	1	0.03	X	43

References

1. X. Gao, T. Xu, C. Shao, Y. Han, B. Lu, Z. Zhang and L. Qu, *J. of Mater. Chem. A*, 2019, **7**, 20574-20578.
2. Q. Lyu, B. Peng, Z. Xie, S. Du, L. Zhang and J. Zhu, *ACS Appl. Mater. Interfaces*, 2020, **12**, 57373-57381.
3. M. J. Li, L. Zong, W. Q. Yang, X. K. Li, J. You, X. C. Wu, Z. H. Li and C. X. Li, *Adv. Funct. Mater.*, 2019, **29**, 1901798.
4. Z. Li, J. Wang, L. Dai, X. Sun, M. An, C. Duan, J. Li and Y. Ni, *ACS Appl. Mater. Interfaces*, 2020, **12**, 55205-55214.
5. C. Wang, S. S. Tang, B. X. Li, J. C. Fan and J. Zhou, *Chem Eng J*, 2023, **455**, 140568.
6. J. C. Zhang, Y. Hou, L. R. Lei and S. Q. Hu, *J. Membrane Sci.*, 2022, **662**, 120962
7. K. Zhang, X. Li, C. Yan, R. Shi, Z. Fang, S. Zhou, R. Cao and J. Tian, *ACS Nano*, 2024, **18**, 10259-10269.
8. X. Xie, X. Wang, Y. Zhang, L. Fang, J. Feng, S. Liu, D. Yu, F. Zhu and X. Chen, *ACS Appl. Mater. Interfaces*, 2024, **16**, 3279-3288.
9. J. Youm, S. H. Lee, I. H. Cho, D. Jeong, J. Bang, H. H. Park and M. S. Kim, *Surf. Interfaces*, 2023, **38,** 102853.
10. J. Chen, Y. Li, Y. Zhang, D. Ye, C. Lei, K. Wu and Q. Fu, *Adv. Funct. Mater.*, 2022, **32**, 2203666
11. J. Tan, S. Fang, Z. Zhang, J. Yin, L. Li, X. Wang and W. Guo, *Nat. Commun.*, 2022, **13**, 3643.
12. L. Huang, Y. Tang, W. Liu, Q. Hu and X. Wei, *Carbohydr. Polym.*, 2024, **326**, 121649.
13. H. Zhong, S. Wang, Z. Wang and J. Jiang, *Chem. Eng. J.*, 2024, **486,** 150203.
14. R. Zhang, R. Zheng, Z. Zheng, Q. Chen, N. Jiang, P. Tang, H. Wang and Y. Bin, *Int. J. Biol. Macromol.*, 2024, **263**, 130022.
15. L. Y. Yang, L. Zhang and D. P. Sun, *ACS Appl. Mater. Inter.*, 2022, **14**, 53615–53626
16. P. Wen, J. Ren and S. J. Ling, *ACS Appl. Electron. Mater.*, 2023, **5**, 2082-2092.
17. X. Han, W. H. Zhang, X. P. Che, L. F. Long, M. J. Li and C. X. Li, *J. of Mater. Chemistry A*, 2022, **10**, 8356-8363.
18. T. Chen, D. L. Zhang, X. Z. Tian, S. Qiang, C. Sun, L. Dai, M. Y. Zhang, Y. H. Ni and X. Jiang, *Carbohyd. Polym.*, 2022, **294**, 119809.
19. X. Liu, H. Gao, J. E. Ward, X. Liu, B. Yin, T. Fu, J. Chen, D. R. Lovley and J. Yao, *Nature*, 2020, **578**, 550-554.
20. J. Liu, L. Huang, W. He, X. Cai, Y. Wang, L. Zhou and Y. Yuan, *Nano Energy*, 2022, **102**, 107709.
21. S. Mandal, S. Roy, A. Mandal, T. Ghoshal, G. Das, A. Singh and D. K. Goswami, *ACS Appl. Electron. Mater.*, 2020, **2**, 780-789.
22. R. Zhu, Y. Zhu, L. Hu, P. Guan, D. Su, S. Zhang, C. Liu, Z. Feng, G. Hu, F. Chen, T. Wan, X. Guan, T. Wu, R. Joshi, M. Li, C. Cazorla, Y. Lu, Z. Han, H. Xu and D. Chu, *Energ. Environ. Sci.*, 2023, **16**, 2338-2345.
23. X. Liu, T. Ueki, H. Gao, T. L. Woodard, K. P. Nevin, T. Fu, S. Fu, L. Sun, D. R. Lovley and J. Yao, *Nat. Commun.*, 2022, **13**, 4369.
24. G. Ren, Q. Hu, J. Ye, X. Liu, S. Zhou and Z. He, *Chem. Eng. J.*, 2022, **441**,135921.
25. Q. Zhao, Y. Jiang, Z. Duan, Z. Yuan, J. Zha, Z. Wu, Q. Huang, Z. Zhou, H. Li, F. He, Y. Su, C. Tan and H. Tai, *Chem. Eng. J.*, 2022, **438**,135588.
26. Z. Wang, J. Li, C. Shao, X. Lin, Y. n. Yang, N. Chen, Y. Wang and L. Qu, *Nano Energy*, 2021, **90**, 106529.
27. R. Zhang, H. Wang, M. Qu, S. Li, Y. Ma, X. Li, P. Tang and Y. Bin, *Chem. Eng. J.*, 2023, **473**, 145325.

28. W. Q. Yang, L. L. Lv, X. K. Li, X. Han, M. J. Li and C. X. Li, *ACS Nano*, 2020, **14**, 10600-10607.
29 T. He, H. Wang, B. Lu, T. Guang, C. Yang, Y. Huang, H. Cheng and L. Qu, *Joule*, 2023, **7**, 935-951.
30. Z. Sun, L. Feng, X. Wen, L. Wang, X. Qin and J. Yu, *Mater. Horiz.*, 2021, **8**, 2303-2309.
31. H. Zhang, N. He, B. Wang, B. Ding, B. Jiang, D. Tang and L. Li, *Adv. Mater.*, 2023, **35**, e2300398.
32. Y. Huang, K. Zhou, H. Cheng, T. He, H. Wang, J. Bai, C. Yang, T. Guang, H. Yao, F. Li, G. Hou, Z. Xu and L. Qu, *Adv. Funct. Mater.*, 2023, **34**, 2308620.
33. Z. Sun, X. Wen, S. Guo, M. Zhou, L. Wang, X. Qin and S. C. Tan, *Nano Energy*, 2023, **116**, 108748.
34. W. He, H. Wang, Y. Huang, T. He, F. Chi, H. Cheng, D. Liu, L. Dai and L. Qu, *Nano Energy*, 2022, **95**, 107017.
35. H. Cheng, Y. Huang, F. Zhao, C. Yang, P. Zhang, L. Jiang, G. Shi and L. Qu, *Energ. Environ. Sci.*, 2018, **11**, 2839-2845.
36. Y. Zhang, T. Yang, K. Shang, F. Guo, Y. Shang, S. Chang, L. Cui, X. Lu, Z. Jiang, J. Zhou, C. Fu and Q. C. He, *Nat. Commun.*, 2022, **13**, 3484.
37. Y. Huang, H. Cheng, C. Yang, H. Yao, C. Li and L. Qu, *Energ. Environ. Sci.*, 2019, **12**, 1848-1856.
38. F. Chen, S. Zhang, P. Guan, Y. Xu, T. Wan, C. H. Lin, M. Li, C. Wang and D. Chu, *Small*, 2023, 2304572.
39. K. Fan, M. Peng, J. Liu, X. Li, X. Wang, B. Kong and X. Liu, *Chem Eng J*, 2023, **461**.
40. X. Wen, Z. Sun, X. Xie, Q. Zhou, H. Liu, L. Wang, X. Qin and S. C. Tan, *Adv. Funct. Mater.*, 2023, **34**, 2311128.
41. X. Zhang, Y. Wang, X. Zhang, C.-W. Lou, J.-H. Lin and T.-T. Li, *Chem. Eng. J,*. 2023, **465**, 142582.
42. D. Shen, M. Xiao, G. Zou, L. Liu, W. W. Duley and Y. N. Zhou, *Adv. Mater.*, 2018, **30**, e1705925.
43. C. Xu, C. Fu, Z. Jiang, T. Yang and M. Xin, *ACS Appl. Nano Mater.*, 2023, **6**, 5930-5938.